

Supporting Information

Disorder-dependent Li diffusion in $\text{Li}_6\text{PS}_5\text{Cl}$ investigated by machine learning potential

Jiho Lee,^{†,§} Suyeon Ju,^{†,§} Seungwoo Hwang,[†] Jinmu You,[†] Jisu Jung,[†] Youngho Kang,^{,‡} and
Seungwu Han^{*,†,¶}*

[†]Department of Materials Science and Engineering, Seoul National University, Seoul 08826, Korea.

[‡]Department of Materials Science and Engineering, Incheon National University, Incheon 22012, Korea

[¶]Korea Institute for Advanced Study, Seoul 02455, Korea.

§J.L. and S.J. equally contributed to this work

* Corresponding authors: youngho84@inu.ac.kr and hansw@snu.ac.kr

Derivation of the ideal relative standard deviation (RSD) of diffusion coefficient in a random walk system

Assuming that the displacement in the x , y , and z directions (X , Y , and Z , respectively) follow independent Gaussian distributions with a mean value of 0 and a standard deviation of σ at each step, the variance increases linearly with time t ,

$$X = \mathcal{N}(0, t\sigma^2), \quad Y = \mathcal{N}(0, t\sigma^2), \quad Z = \mathcal{N}(0, t\sigma^2).$$

The mean and variance of the squared displacement in the x direction are obtained as follows:

$$E[X^2] = \text{Var}[X] + E[X]^2 = t\sigma^2,$$

$$E[X^4] = \frac{\int_{-\infty}^{\infty} x^4 e^{-x^2/2t\sigma^2} dx}{\int_{-\infty}^{\infty} e^{-x^2/2t\sigma^2} dx} = 3t^2\sigma^4,$$

$$\text{Var}[X^2] = E[X^4] - E[X^2]^2 = 3t^2\sigma^4 - t^2\sigma^4 = 2t^2\sigma^4.$$

Since X , Y , and Z are independent of each other, the mean and variance of the squared displacement in the three dimensions (R^2) are obtained as the sum of the mean and variance in each direction,

$$E[R^2] = 3t\sigma^2, \quad \text{Var}[R^2] = 6t^2\sigma^4.$$

In an N -atom system, the variance of the mean squared displacement (MSD) is reduced to $1/N$, and the standard deviation of the MSD in an N -atom system is

$$\sqrt{6t^2\sigma^4 \times \frac{1}{N}}.$$

Finally, the mean and standard deviation of the diffusion coefficient (D) are expressed as

$$E[D] = 3t\sigma^2 \times \frac{1}{6t} = \frac{\sigma^2}{2}, \quad \text{Std}[D] = \sqrt{6 \times \frac{1}{N} \times t\sigma^2 \times \frac{1}{6t}} = \frac{\sigma^2}{\sqrt{6N}},$$

and the relative standard deviation (RSD) of the diffusion coefficient in a random walk system can be obtained as follows:

$$\text{RSD}[D] = \frac{\text{Std}[D]}{E[D]} = \frac{\sqrt{2}}{\sqrt{3N}}.$$

Since only lithium ions are free to move in a solid electrolyte system, we consider the number of Li ions in the supercell as the number of random walk particles. The number of Li ions in the $2 \times 2 \times 2$, $3 \times 3 \times 3$, $4 \times 4 \times 4$, and $5 \times 5 \times 5$ supercells are 192, 648, 1536, and 3000, respectively. Therefore, the ideal RSDs of diffusion coefficient are 0.059, 0.032, 0.021, and 0.015 respectively. It should be noted that, based on the Nernst-Einstein equation, the RSD of Li conductivity is equivalent to the RSD of the diffusion coefficient.

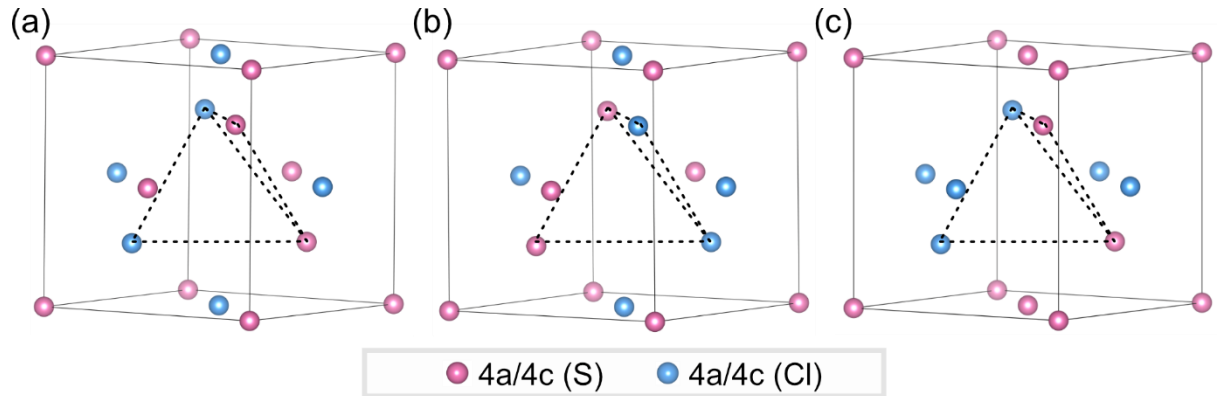


Figure S1. The two possible S/Cl configurations in the unit cell. (a) and (b) show the same configuration from different views, while (c) shows the second configuration. The vertices of the tetragonal indicate 4c sites, and the remaining sites correspond to 4a sites.

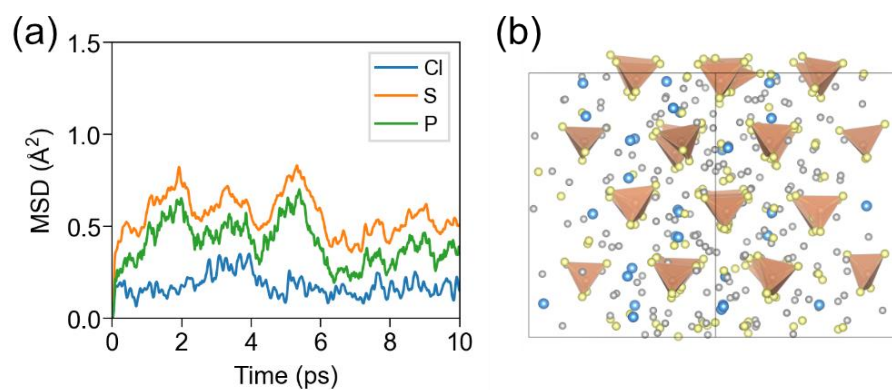


Figure S2. (a) The elemental MSD of 1200 K AIMD training trajectories. (b) The snapshot of the final structure.

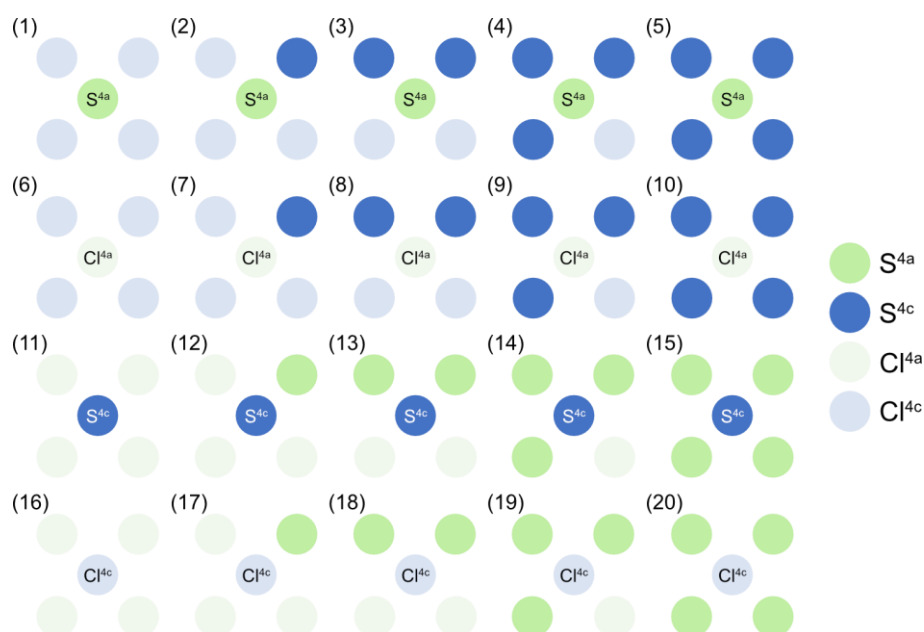


Figure S3. Possible 20 local structures within the neural network cutoff. The cases (10), (15), and (20) are excluded in the molecular dynamics portion of the training set.

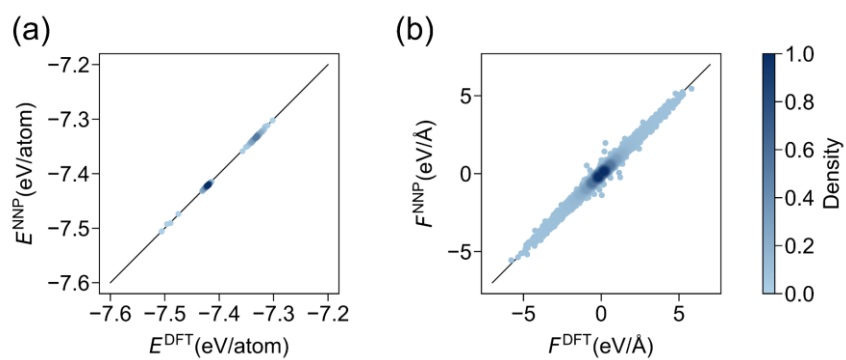


Figure S4. (a) Energy and (b) force correlation of DFT and NNP. The value 1.0 in the density color bar represents the densest point of the data and the value 0.0 the least.

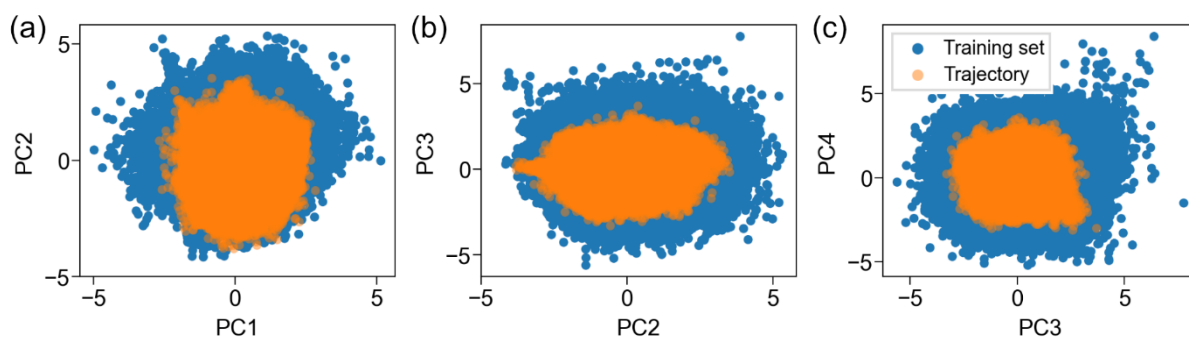


Figure S5. The principal component analysis of the training set and the 500 K NNP-MD trajectories. (a) Principal axis 1 versus principal axis 2 (b) Principal axis 2 versus principal axis 3 (c) Principal axis 3 versus principal axis 4.

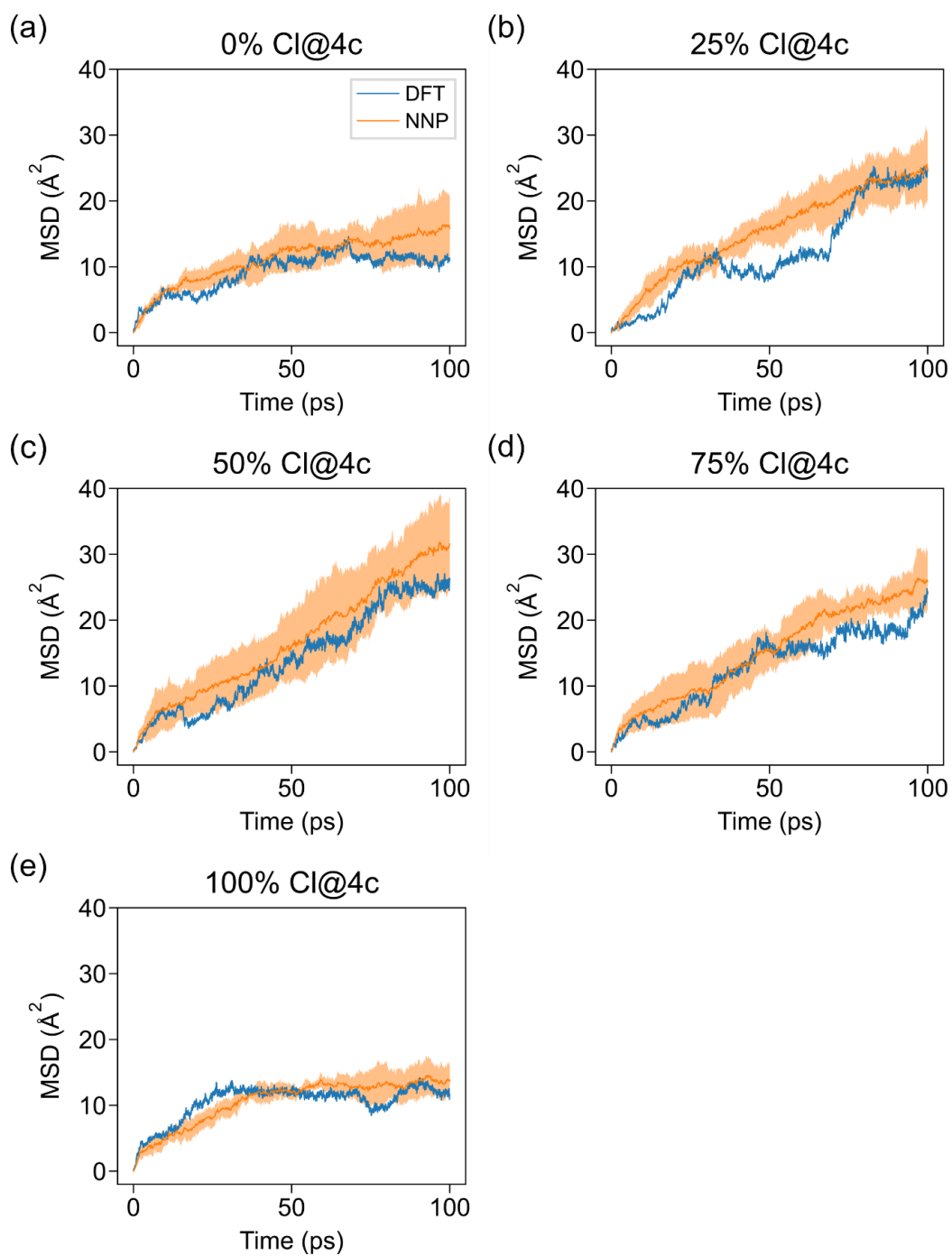


Figure S6. 500 K MSD plot of both DFT (blue) and NNP (orange) on unit cells with (a) 0%, (b) 25%, (c) 50%, (d) 75%, and (e) 100% Cl@4c. For NNP, the lines indicate the average MSD of 5 simulations, and shades represent the standard deviation.

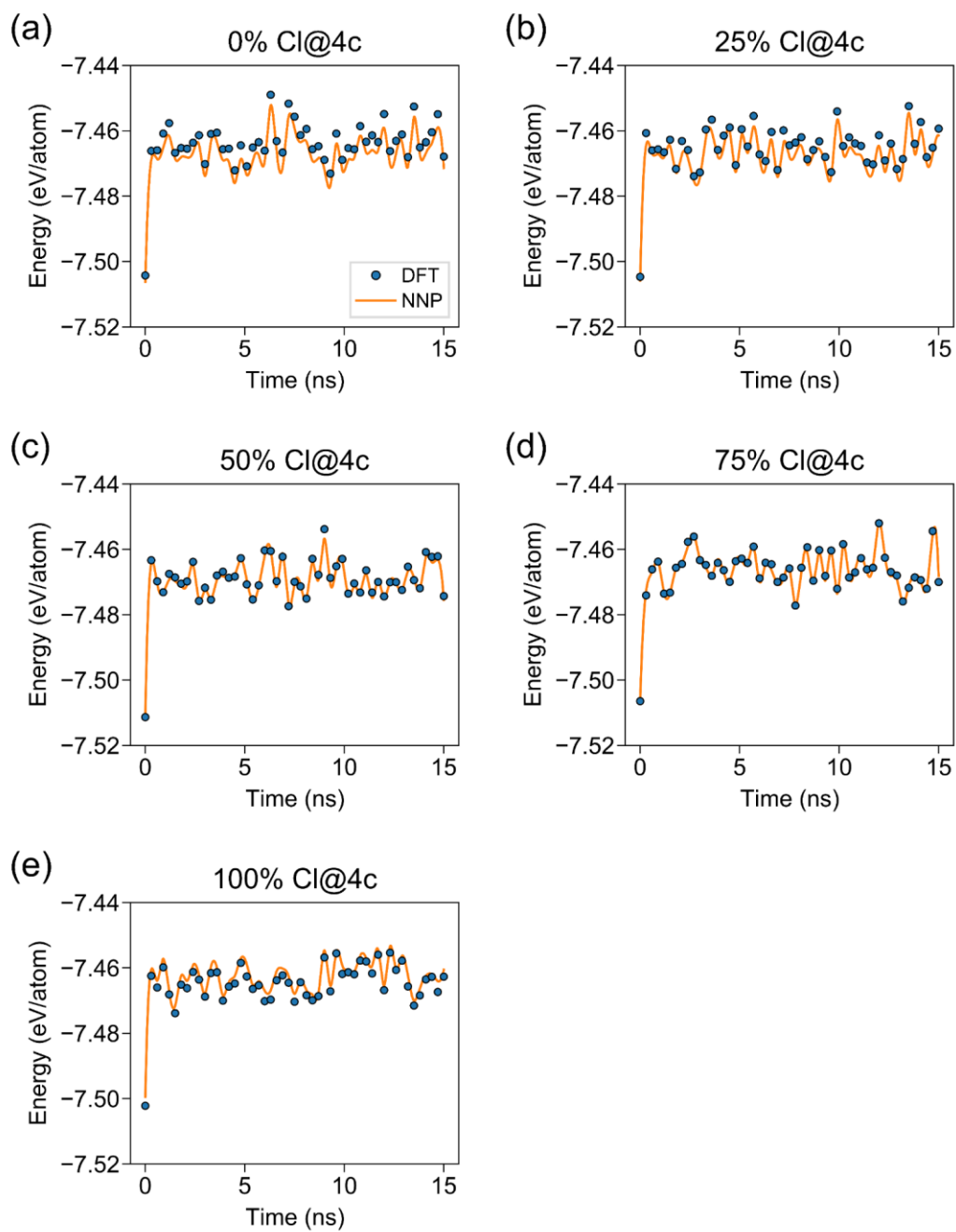


Figure S7. 300 K NNP-MD simulation (orange) and DFT single-point calculations (blue) on unit cells with (a) 0%, (b) 25%, (c) 50%, (d) 75%, and (e) 100% Cl@4c. For each disorder, 50 structures are selected to calculate DFT static energies from 15 ns NNP-MD trajectory.

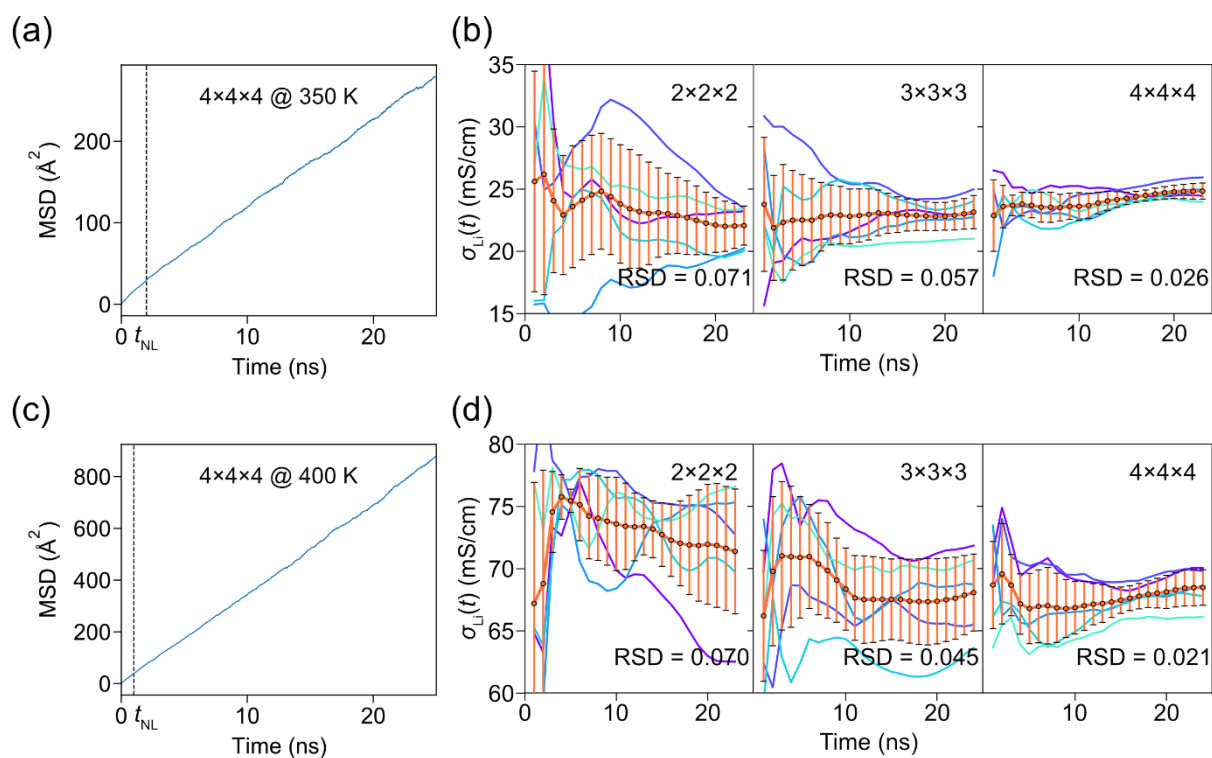


Figure S8. MSD(t) of 50% Cl@4c 4x4x4 supercell performed at (a) 350 and (c) 400 K. Li conductivities of 5 individual simulations with the same Cl@4c but different Li distributions (blue colors) and the average and standard deviation of 5 simulations (orange) at (b) 350 and (d) 400 K.

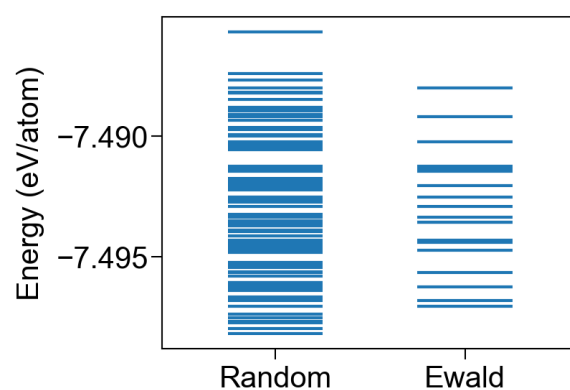


Figure S9. The energy range of structures from random and Ewald summation methods evaluated by NNP. A total of 100 random structures were generated with varying S/Cl and Li arrangements in $2 \times 2 \times 2$ supercells. Among them, the 20 lowest Ewald energy structures were selected and labeled as “Ewald”.

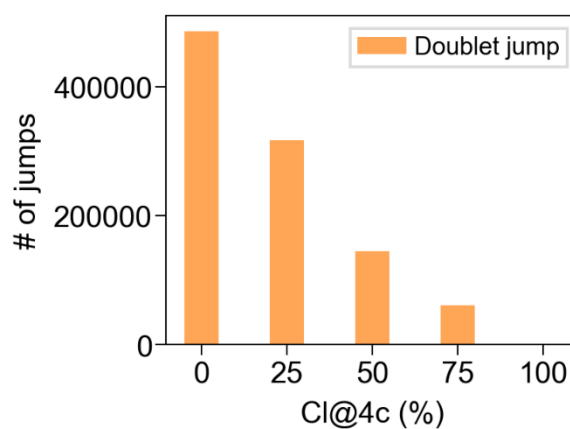


Figure S10. The total number of doublet jumps that occur over 25 ns at 300 K for various Cl@4c percentages.

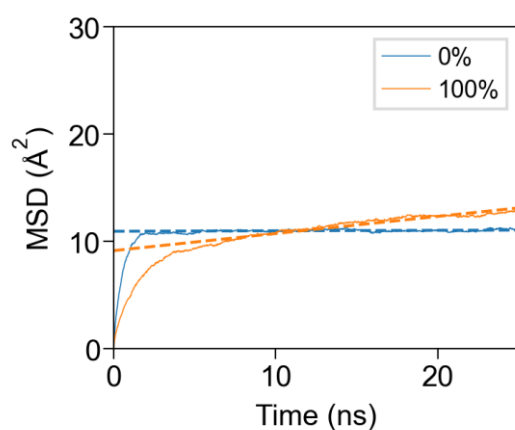


Figure S11. MSD(t) plot for 0% and 100% Cl@4c. The dashed lines indicate curve fitting for the linear regions of 0% and 100% Cl@4c.

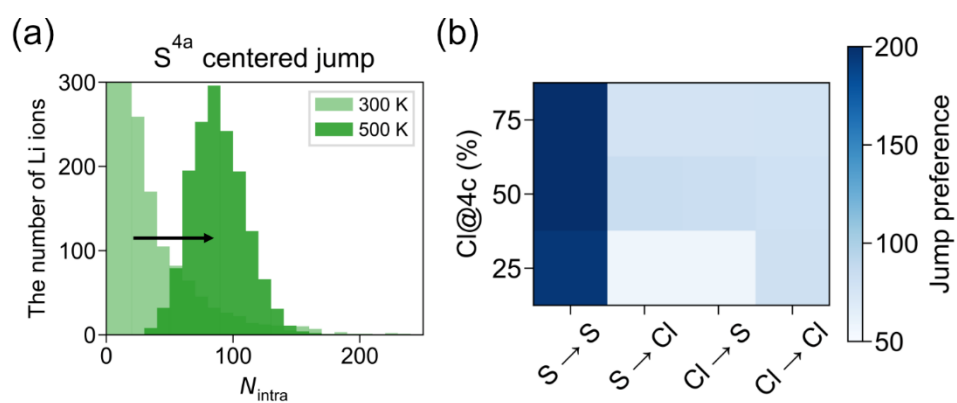


Figure S12. (a) Increase of S^{4a} -centered jump at 500 K compared to 300 K. (b) Jump preference for 4 types of inter-cage jumps with respect to Cl@4c performed at 500 K.

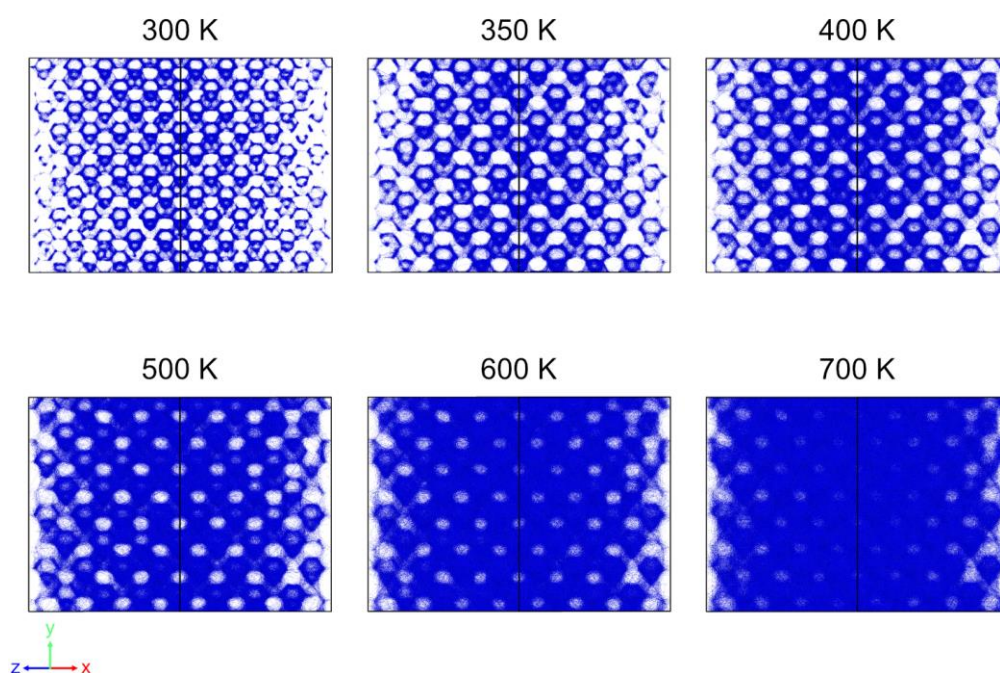


Figure S13. Trajectories of Li atoms calculated at 300, 350, 400, 500, 600, and 700 K during initial 10-ns MD simulations with 50% Cl@4c.

Cl@4c (%)	Type	Settings	Number of structures	Number of atoms in a structure	Number of atomic environments
0	Bulk crystals	$\pm 5\%$ strain	11	416	4,576
50			33	416	13,728
100			11	416	4,576
50	AIMD	600 K	970	416	403,520
		1200 K	970	416	403,520
Total		-	1,995	-	829,920

Table S1. Details of the training set.

No.	η	R_s	λ	ζ
G^{radial}				
1	0.003214	0	-	-
2	0.035711	0	-	-
3	0.071421	0	-	-
4	0.124987	0	-	-
5	0.214264	0	-	-
6	0.357106	0	-	-
7	0.714213	0	-	-
8	1.428426	0	-	-
G^{angular}				
9	0.000357	-	-1	1
10	0.000357	-	-1	2
11	0.000357	-	-1	4
12	0.000357	-	1	1
13	0.000357	-	1	2
14	0.000357	-	1	4
15	0.028569	-	-1	1
16	0.028569	-	-1	2
17	0.028569	-	-1	4
18	0.028569	-	1	1
19	0.028569	-	1	2
20	0.028569	-	1	4
21	0.089277	-	-1	1

22	0.089277	-	-1	2
23	0.089277	-	-1	4
24	0.089277	-	1	1
25	0.089277	-	1	2
26	0.089277	-	1	4

Table S2. Details of hyperparameters of atom-centered symmetry function. The cutoff radius is 6.0 Å for both radial and angular terms.

	$\sigma_{10\% \text{ Cl@4c}}$ (mS/cm)	$\sigma_{25\% \text{ Cl@4c}}$ (mS/cm)	$\sigma_{50\% \text{ Cl@4c}}$ (mS/cm)	$\sigma_{75\% \text{ Cl@4c}}$ (mS/cm)
Simulation 1	4.20	6.07	5.55	4.22
Simulation 2	4.75	6.64	4.85	4.20
Simulation 3	4.78	6.61	5.22	4.25
Mean	4.56	6.44	5.21	4.22
Standard deviation	0.27	0.26	0.29	0.02

Table S3. The Li-ion conductivity (σ_{Li}) of structures with 10%, 25%, 50%, and 75% Cl@4c on three individual simulations.